Applications of AdS/CFT to strongly correlated matter: from numerics to experiments

Chagnet, N.

Chapter 1

Introduction

1.1 Quantum critical points and strongly correlated electrons

Within the last century, Condensed Matter Theory (CMT) has emerged as one of the most successful areas of physics. The initial impetus behind it was the statistical mechanics underpinning of thermodynamics which opened the door to understanding the solid and liquid phases of matter made out of atoms and bound together through the electromagnetic force. With the advent of quantum mechanics, modern solid state physics was born, and the field grew to the more general study of quantum many-body systems.

A key pillar of CMT is *symmetries*; within Landau's framework, phases of matter are categorized by their symmetries and described by a low energy effective functional constrained by these symmetries. As an example, the effective quantum many-body description of up-down spins can be done through the following free energy functional

$$\mathcal{F}[\psi] = \frac{s(T)}{2}\psi^2 + \frac{u(T)}{4}\psi^4 + \dots \,, \tag{1.1}$$

where ψ is a real scalar field modelling the average number of up (positive) and down (negative) spins in some local area, also called *the magnetization*. A priori, the coefficients s and u depend on the temperature T and other physical parameters of the system. The symmetry under which the action (1.1) is invariant is $\mathbb{Z}_2$ inversion *i.e.*, when all spins simultaneously flip their signs $\psi \to -\psi$. When this symmetry is broken, either explicitly by interactions or spontaneously by the state, the physical system undergoes a *phase transition*. In our Ising example, the former can be done by coupling to an external magnetic field $\mathcal{F}_{\text{explicit}}[\psi] = \mathcal{F}[\psi] + h\psi$, which explicitly breaks the $\mathbb{Z}_2$

invariance. The case of spontaneous breaking can be understood as the deformation of the energy functional when tuning temperature. When $s(T) > 0$ and $u(T) > 0$, $\mathcal{F}$ has a single minimum at $\psi = 0$ (the state is called a paramagnet) while when $s(T) < 0$ and $u(T) > 0$, two minima emerge at $\psi = \pm\sqrt{\frac{-s}{u}} \neq 0$ (the state is then a ferromagnet).[1] In the last case, since $\psi \neq 0$, the $\mathbb{Z}_2$ invariance is broken by the state while the functional remains invariant under the symmetry.

This scenario of spontaneous symmetry breaking presents a continuous transition where the system passes through a *critical point* at $s(T = T_c) = s_c$ ($s_c = 0$ for our Ising example). The self-induced change is driven by thermal fluctuations. At the critical point, the correlation length ξ diverges and the correlation functions showcase an emergent scale invariance — the system is then described by a conformal field theory (CFT). If the system depends on other physical parameters (*e.g.*, pressure, chemical potential, etc.) collectively denoted by p, one can tune the transition at zero temperature to a critical point located at $s(p = p_c, T = 0)$. The system is now driven by quantum fluctuations instead of thermal fluctuations and the critical point is called a quantum critical point (QCP). It is this type of quantum phase transition (QPT) where the corresponding CFT exists at temperatures close to zero that will be of relevance to this thesis.

Most systems one encounters in CMT are generally perturbative in nature; they are usually related to a free system by a small deformation, an adiabatic deformation (*e.g.*, the Fermi liquid is adiabatically connected to the Fermi gas) or by some duality (*e.g.*, the bosonization of the Luttinger liquid). In these cases, the excitations of the systems are particle-like in nature and are called *quasiparticles*. For interacting systems, these quasiparticles generally acquire a finite yet large enough lifetime such that the quasiparticle manifests itself as a well-defined resonance peak in the spectrum of the correlation functions. The dynamics of the system can then be understood in terms of the collisions of these quasiparticles.

One of the most interesting properties of QCPs is that the excitations of the system at that point are generically not quasiparticles. Consider the following Euclidean action as a toy model [1]

$$S_{\mathrm{QCP}}(\psi) = \int \mathrm{d}^2x\mathrm{d}\tau \left[(\partial_\tau \psi)^2 + (\nabla\psi)^2 + \frac{s}{2}\psi^2 + \frac{u}{4}\psi^4 \right] , \tag{1.2}$$

This action is a generalization of the Ising functional (1.1) and will describe the Ising QPT between the previously described ferromagnetic and paramagnetic phases. Away from the QCP, both of these phases have quasiparticle excitations called *magnons*. How do we describe the theory *at criticality*, where there are no quasiparticles? In dimensions $d > 3$, one can still get away with a quasiparticle description (in a free field representation) even though formally there are no such excitations. In $2+1$ dimensions,

[1] Note that the case of $u(T) < 0$ yields an unbounded energy functional as $|\psi| \to \infty$ and therefore signals an unphysical instability.

however, it is well-known that under Renormalization Group (RG) flow, the ψ^4 theory admits not only the trivial Gaussian fixed point $u = s = 0$ but also the Wilson-Fisher fixed point characterized by $(s^\star, u^\star)$ — in that case this non-trivial fixed point will be the location of the Ising QCP. At this QCP, the two-point correlator for ψ will then take the conformal form [1]

$$G_{\psi\psi}(\omega, k) \sim \frac{1}{\left(k^2 - \omega^2\right)^{(2-\eta)/2}} \tag{1.3}$$

where $\eta \neq 0$ is some anomalous scaling exponent for ψ. Would $\eta = 0$ have been true, then the propagator would have poles at $\omega = \pm k$, and we would recover a quasiparticle description of the system.[2] However, for generic values of η, the propagator is not an analytic function and exhibits branch cuts instead of well-defined poles — this is the simplest example of 'unparticle' physics.

By definition, at the critical point, the correlation length ξ diverges as $\xi \sim |s - s_c|^{-\nu}$, defining the critical exponent ν. If we now add a small temperature, we still expect the system to remember its critical origin and therefore the correlator should take the scaling form

$$G_{\psi\psi}(\omega, k) \sim T^{\frac{\eta-2}{\mathbf{z}}} \mathcal{F}\left(\frac{k}{T^{1/\mathbf{z}}}, \frac{\xi^{-1}}{T^{1/\mathbf{z}}}, \frac{\omega}{T}\right). \tag{1.4}$$

In the previous equation, we have allowed for a dynamical critical exponent $\mathbf{z}$ which accounts for a different scaling of time and space. Since the action (1.2) is manifestly Lorentz invariant, then $\mathbf{z} = 1$. However, other theories can a priori show a non-trivial emergent $\mathbf{z} > 1$.[3] From the correlator (1.4), we can see that for temperatures $T > \xi^{-\mathbf{z}}$, then the scaling ratio $T\xi^{\mathbf{z}}$ remains large (and even grows with increasing T) and thus the physics of the system is controlled by the fluctuations of the QCP ground state. This is a special phase of the system called the quantum critical regime, which, remembering the scaling of ξ, is then defined at low temperatures by the region $T > |s - s_c|^{\mathbf{z}\nu}$. In Fig. 1.1, we draw a schematic phase diagram for the system described by (1.2) where the quantum disordered phase is the paramagnet and the quantum ordered phase is the ferromagnet (which eventually transitions back to a classical paramagnet at high-enough temperature). A QCP without a quasiparticle description

[2] In this case, the poles have no imaginary part, so these quasiparticles do not decay.

[3] This is for instance the case for the Hertz-Millis model [2, 3] describing the coupling of a bosonic order parameter ψ passing through a QCP and coupled to fermionic excitations. After integrating out the fermions, we are left with an effective action for the critical boson of the form

$$S = \int \mathrm{d}\omega \mathrm{d}^d q \left[\left(\frac{|\omega|}{\gamma(q)} + q^2\right)|\psi|^2 + m^2|\psi|^2 + \ldots\right] \tag{1.5}$$

where we ignored irrelevant terms for simplicity. If the critical boson describes a ferromagnetic order parameter, then $\gamma(q) \sim |q|$ and therefore the emergent dynamical critical exponent at this QCP is $\mathbf{z} = 3$. Note that while the Hertz-Millis model predicts generic mean-field exponents below the upper-critical dimension $d_c = 1$, there are subtleties in two- and three-dimensional systems which may invalidate this simple Ginzburg-Landau description [4, 5, 6].

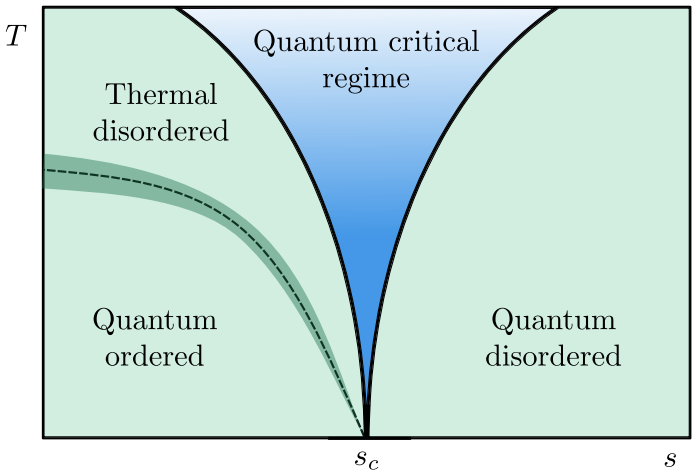

Figure 1.1: Schematic phase diagram of a system in the presence of a quantum critical point. On each side of the transition, there is a quantum ordered and disordered phase which can both be described by quasiparticles. The quantum ordered phase admits a classical phase transition to a thermal disordered phase. The shaded area indicates the area where fluctuations along the time direction are frozen, and the behavior is purely classical. At finite temperature, there is a region where the physics of the QCP remains dominant and the excitations of this region cannot be described perturbatively as quasiparticles.

is possibly the best example of a 'strongly interacting' or 'strongly coupled' system, as opposed to the perturbative systems mentioned at the beginning of this introduction which are dominated by quasiparticles.[4]

The explorations of this thesis are motivated by a variety of strongly coupled systems. Among them stands the mysterious 'strange' metallic phase of the copper oxides high-T_c superconductors (or *cuprates*) discovered in the 1980s [8]. Such cuprates are so-called Mott insulators. By tweaking their chemical composition, the number of available charge carriers per ionic site (electron or holes) can be changed (this is called electron or hole doping) and they can become conducting metals which superconduct at low temperature, where the temperature of onset of the superconducting phase changes with the doping parameter. The main characteristic of the cuprates is that for some optimal value of doping p^*, the transition temperature shows an anomalously high maximum, orders of magnitude larger than that predicted by the conventional Bardeen–Cooper–Schrieffer (BCS) theory (where $T_c^{\max} \simeq 35\,\mathrm{K}$, see Fig. 1.2). This, in essence, shows that such cuprates do not reflect the physics of conventional Fermi

[4] Note that this widely used nomenclature is not entirely exact. Adiabatically deformed systems can be strongly interacting and still have quasiparticle excitations. (see *e.g.*, for the Fermi liquid [7]). In this thesis we will follow this naming convention in spite of this technicality to match the rest of the literature.

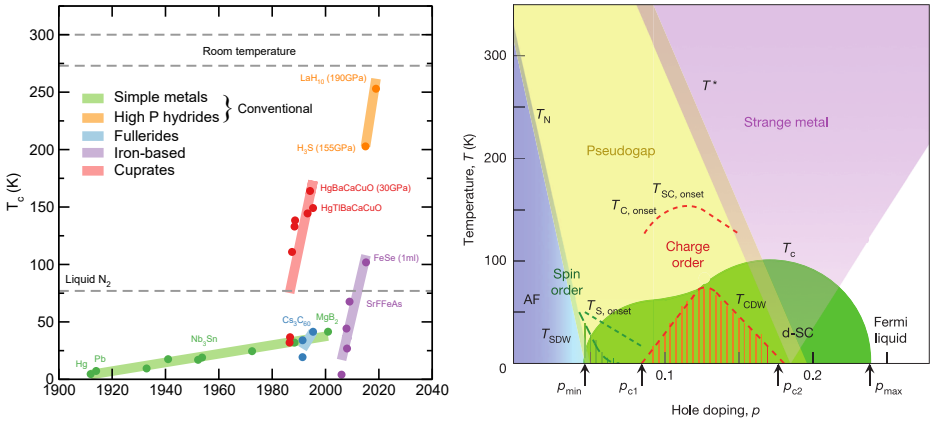

(a) Figure taken from [9]. (b) Figure taken from [10].

Figure 1.2: (a) Graph plotting the history of discovery of high-T_c superconductors. In green are the conventional superconductors described by BCS theory while in red are the cuprates. (b) Generic phase diagram of the cuprates parametrized by hole doping and temperature.

liquid quasiparticles.

The superconducting phase is not the only interesting part of these materials: the phase diagram of cuprates shows a remarkable number of exotic phases, with a pseudo-gap phase at low doping and a regular Fermi liquid phase at large doping. Yet the phase where the non-quasiparticle nature is most manifest is the *strange metal* phase at optimal doping, at temperatures above the superconducting transition. This phase is characterized by a variety of properties, the most prominent of which is the linear-in-T resistivity ρ — where a regular Fermi liquid metal would have $\rho \sim T^2$ at low temperatures. This linear-in-T resistivity is valid not only at low temperatures but also throughout a large range of temperatures where other interactions would usually take dominance (*e.g.*, the $\rho \sim T^5$ electron-phonon contribution in regular metals is absent in strange metals). Moreover, at large enough temperature, the resistivity of a metal whose transport is mediated via quasiparticles should saturate at the Mott-Ioffe-Regel (MIR) bound [10]. Yet in strange metals, that bound is violated by the linear-in-T resistivity (Fig. 1.3a, see also [11, 12]) indicating again that the quasiparticle description of electronic transport should break down in those systems.

While early efforts were focused on attributing this behavior to the underlying high-T_c physics in cuprates, it was demonstrated that such strange metals can be found in more general strongly correlated electronic systems [14, 15]. It indicated that more universal physics could be at the root. One clear candidate for non-quasiparticle physics is the existence of a QCP, hidden by the superconducting dome, with the strange metallic physics originating from the quantum critical regime [16, 10].

In strange metals, experiments have shown, however, that if quantum critical

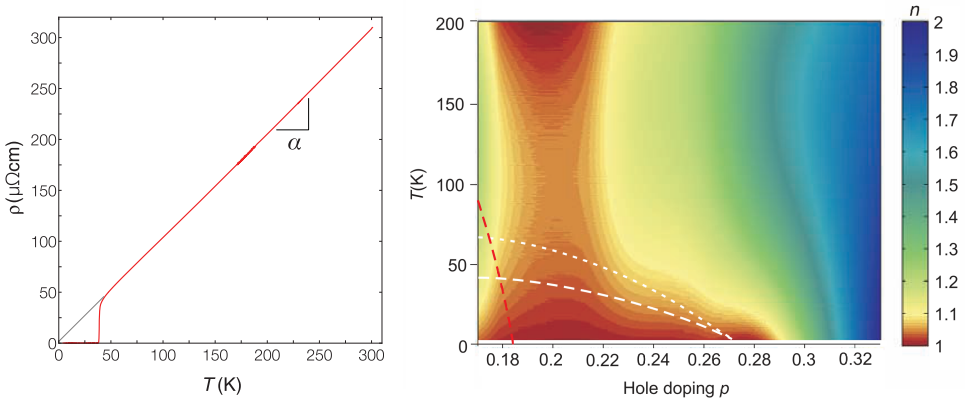

(a) Figure taken from [11].

(b) Figure taken from [13].

Figure 1.3: In-plane resistivity of the hole-doped $La_{2-p}Sr_pCuO_4$ (LSCO) cuprates. (a): We see the resistivity violates the MIR bound (located between 200 K and 300 K) at large temperature indicating transport is not mediated via quasiparticles. The hole-doping parameter is $p = 0.19$. (b): Exponent n of the resistivity $\rho \sim T^n$ as a function of hole-doping. The red region indicates the strange metallic phase where $n \simeq 1$. The data within the superconducting dome is obtained via extrapolation of finite magnetic field data.

physics is at the origin of this phenomenon, it is not simply a QCP, but the even more exotic case of a quantum critical phase (QCPh), a continuous set of QCPs connected by a line. This is supported by measurements of the effective exponent n for the in-plane resistivity in cuprates $\rho \sim T^n$ [13] (in the presence of a high magnetic field such that the superconducting phase is suppressed and thus the hidden part of the resistivity can be extrapolated). This is represented in Fig. 1.3b where we see indeed that the strange metallic behavior does not seem to converge to a point but to a finite segment at zero temperature. Another argument in support of a QCPh can be found in ARPES measurements showing that the imaginary part of the electron-like non-quasiparticle self-energy[5] takes the form $\Sigma(\omega) - \Sigma(0) \sim \left[T^2 + \omega^2\right]^{\alpha}$ with, crucially, α a non-integer value that varies continuously with hole doping p [17]. The key difference between a QCP and a QCPh is that in the latter case, some constraint must allow the emergent critical boson to be gapless within a finite range of parameter space instead of at a specific point.[6] The coupling of this critical boson with a Fermi surface allows for non-Fermi liquid behavior in the photoemitted electron self-energy. This persistent gaplessness over a range of parameters is responsible for the continuous dependence of critical exponents to the tuning parameter instead of a fixed value but remains a big mystery from a theoretical point of view. A core objective of this thesis will be to show that, surprisingly, quantum critical phases naturally arise in the so-called 'holographic'

[5] In the language of our toy model, the self-energy is just the correction to the dispersion relation of the quasiparticle pole due to interactions.

[6] We refer the reader to this excellent review for a more in-depth discussion of quantum critical phases [18].

description of quantum critical states [18] — which makes it a fertile ground to look for theories in the same universality class as observed strongly coupled non-quasiparticle and/or QCP-type physics, and will be the subject of our focus starting from now.

1.2 The holographic AdS/CFT correspondence

One of the breakthroughs in describing non-quasiparticle-like physics has been the discovery of the AdS/CFT correspondence, also known as holographic duality. Many books and reviews have been written on the topic already and more details can be found within those texts [19, 20, 1, 21]. Given the sizeable length such an in-depth introduction requires, it is not the goal of this section to exhaustively review the topic, but rather to introduce the main arguments and ideas behind applied holography through canonical examples whose details will also serve to highlight common notations and techniques.

The first example of the AdS/CFT duality was brought forth by Juan Maldacena in 1997 within the framework of string theory [22]. This result connects the physics of a very special quantum field theory (QFT) at strong coupling — a CFT which has no quasiparticles — with that of weakly-coupled gravitational physics. While a full derivation of the string theory background required to understand this specific example in details might be too intricate for the scope of this section, we will nonetheless attempt to extract the essential argument behind this matching.

To that end, let us first consider an $O(N)$ vector theory (see [23] for a more in-depth review). We consider a field ϕ_i in a vector representation of the symmetry group $O(N)$. Its dynamics are described by an action invariant under these transformations. Interaction terms inside the action must therefore be $O(N)$ scalars of the form $\phi^2 \equiv \phi \cdot \phi$, $\phi \cdot \partial_\mu \phi$, etc. to lowest orders in ϕ. We can thus build the following Euclidean action

$$S = \int \mathrm{d}^d x \left[\frac{1}{2}(\partial\phi)^2 + \frac{m_0^2}{2}\phi^2 + \frac{g}{2N}(\phi^2)^2 \right] . \tag{1.6}$$

Why the quartic coupling has an extra N factor will become evident in the following derivation. The theory at $g = 0$ is a simple Gaussian free theory with partition function

$$Z_0 \equiv \prod_{i=1}^{N} \int \mathcal{D}\phi_i \, e^{-\frac{1}{2}\int \mathrm{d}^d x \left[(\partial\phi_i)^2 + m_0^2 \phi_i^2\right]} \equiv e^{-N S_0(m_0^2)} , \tag{1.7}$$

where we defined the effective action $S_0(m_0^2) = -\frac{1}{2}\mathrm{Tr}\log\left(-\partial^2 + m_0^2\right)$ of a single scalar field component ϕ_i. Keeping g finite, we apply a Hubbard-Stratanovitch transformation to this model such that we can rewrite the partition function $Z = \int \mathcal{D}\phi e^{-S[\phi]}$ into $Z' = \mathcal{N}\int \mathcal{D}\phi\mathcal{D}\sigma e^{-S'[\phi,\sigma]}$, where $\mathcal{N}$ is an overall normalization term which has no effect on the correlations, with the new action

$$S' = \int \mathrm{d}^d x \left[\frac{1}{2}(\partial\phi)^2 + \frac{m_0^2}{2}\phi^2 - \frac{N}{2g}\sigma^2 + \phi^2\sigma \right] . \tag{1.8}$$

The action S' is again Gaussian in ϕ, and therefore we can apply the computation done previously at $g = 0$ with effective mass $m^2 = m_0^2 + 2\sigma$ such that, after integrating out the vector ϕ, the partition function is $Z_{\text{eff.}} = \mathcal{N} \int \mathcal{D}\sigma e^{-NS_{\text{eff.}}[\sigma]}$ with the effective action

$$S_{\text{eff.}}[\sigma] = S_0(m_0^2 + 2\sigma) - \frac{1}{2g} \int \mathrm{d}^d x \sigma^2 \ . \tag{1.9}$$

Due to the normalization of the quartic coupling in the action (1.6), the path integral now only depends parametrically on the number of vector components N through the overall normalization of the action. In the large-N limit, the path integral will then be dominated by the saddle-point $\sigma_{\text{cl.}}$ defined through the condition $\frac{\delta S_{\text{eff.}}}{\delta \sigma}(\sigma_{\text{cl.}}) = 0$. This condition is equivalent to the implicit (or gap) equation $G_0(x, x; m^2) = \frac{\sigma_{\text{cl.}}}{g}$ where G_0 is the propagator of a free scalar field with mass $m^2 = m_0^2 + 2\sigma_{\text{cl.}}$.

So far, we have shown that for this class of theories, taking a large-N limit can be an effective tool to achieve some semi-classical description where a saddle-point dominates the path integral. However, we see that the vector model is also entirely dominated by the Gaussian fixed point for any finite coupling g. A similar yet richer model can be considered by promoting the field ϕ_i from the vector representation to the adjoint representation of $O(N)$ — Φ_{ij} is now a real symmetric matrix with $\frac{N(N+1)}{2}$ components and the action (1.6) will then be promoted to

$$S = \int \mathrm{d}^d x \left[\frac{1}{2} \operatorname{Tr}\left(\partial \Phi\right)^2 + \frac{m_0^2}{2} \operatorname{Tr} \Phi^2 + \frac{g}{\sqrt{N}} \operatorname{Tr} \Phi^3 \right] \ . \tag{1.10}$$

In the new action (1.10), we only consider the relevant deformation $\operatorname{Tr}\Phi^3$ (in $d = 4$) for simplicity, but there is a priori also a $\operatorname{Tr}\Phi^4$ interaction — as there was in the vector model (the cubic interactions are not present in the vector model due to the $O(N)$ invariance condition). While in the vector model most loop diagrams get suppressed by powers of $1/N$ such that the only leading order effect is to renormalize the scalar mass (see Fig. 1.4), in the matrix model loop diagrams with increasingly high powers of the coupling g remain at leading order in N (see Fig. 1.5). The matrix model can therefore capture more non-trivial physics than the vector model [24]. It is then possible to take the semi-classical limit $N \gg 1$ while keeping the strongly coupled physics of the system. This interplay of limits is controlled by the so-called 't Hooft coupling $\lambda = gN$ such that $\lambda \ll 1$ is akin to a weak coupling limit (similar to the vector model) while $\lambda \gg 1$ is the strong coupling limit.

We can now briefly explain Maldacena's discovery. Within type-IIB string theory, solitonic $3+1$-dimensional defects (so-called $D3$-branes) have a zero-mode sector which is essentially the supersymmetric extension of (1.10). There, the strings connecting the branes are described by the matrix fields Φ_{ij} and the 't Hooft coupling is given by $\lambda \sim g_s N$ with g_s the string coupling constant. This is the low energy theory of a supersymmetric $\mathcal{N} = 4$ $SU(N)$ gauge theory which is a CFT. Maldacena observed that studying the system described by the supersymmetric extension of (1.10) at strong coupling $\lambda \gg 1$ and in the large-N limit $N \gg 1$ has a window $1 \ll \lambda \ll N^2$ within

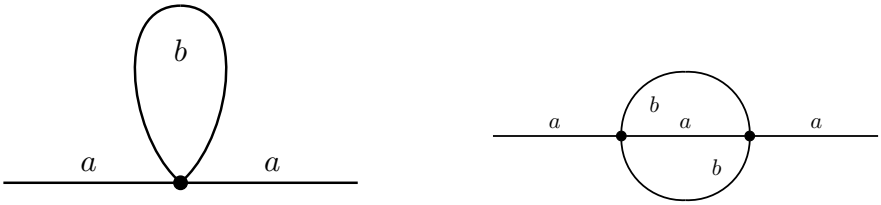

(a) The vertex brings a factor g/N while the loop over the index b yields a factor N. The overall order of this diagram is $\mathcal{O}(g)$.

(b) The vertices bring a factor $(g/N)^2$ while the loop over the index b yield a factor N. The overall order of this diagram is $\mathcal{O}(g^2/N)$.

Figure 1.4: One-loop and two-loop 1PI diagram contributions to the vector model two-point function with equal input/output indices. We see that at two-loop order, the irreducible diagram is subleading in N and thus the leading contribution at every loop order will be the components of the geometric series associated with 1.4a.

perturbative string theory $g_s = \frac{\lambda}{N} \ll 1$ where the gravitational description is weakly coupled, and the gauge description remains strongly coupled. In this limit, the branes form an asymptotically hyperbolic geometry of 5-dimensional Anti-de Sitter (AdS) spacetime times a 5-dimensional sphere. As string theory is a theory of quantum gravity, the string coupling not only sets the coupling of the gauge theory $g^2_{\text{YM}} = \frac{\lambda}{N}$, it also controls the dimensionless gravitational constant $\frac{G_N}{L^8} = \frac{1}{N^2}$, where L is the radius of curvature of the AdS spacetime. In this double limit, L is much larger than the Planck and string lengths *i.e.*, the curvature of the spacetime is weak. Thus, we have a *weakly coupled semi-classical gravitational* description of the system, which is *strongly coupled* from the brane perspective. This is the essence of the holographic principle: the duality maps strongly coupled CFT systems to weakly coupled gravitational systems.

Following on Maldacena's seminal paper, a plethora of similar mappings were found within string theory (see *e.g.*, this review [25]) — this is called the 'top-down' approach. In order for the correspondence to be a practical tool, it is also necessary to find a mathematical formulation of the correspondence. This was put forward through the Gubser-Klebanov-Polyakov-Witten (GKPW) formula [26, 27] which relates the generating functional of a $d+1$-dimensional CFT to the gravitational partition function in AdS in one dimension higher

$$\int \mathcal{D}\mathcal{O}\, e^{iS_{\text{QFT}}[\mathcal{O}]+i\int \mathrm{d}^{d+1}x h_i(x)\mathcal{O}_i(x)} = \int_{\phi_i(r=\infty,x)=h_i(x)} \mathcal{D}\phi\, e^{iS_{\text{grav.}}[\phi]}\,. \tag{1.11}$$

From this formula, we see that each operator $\mathcal{O}$ of the CFT is dual to the asymptotic boundary value of some bulk field ϕ in a gravitational AdS spacetime with one extra dimension (named the radial direction and denoted by r). An AdS spacetime is different from flat spacetime where one usually requires fields vanish infinitely far away. Instead,

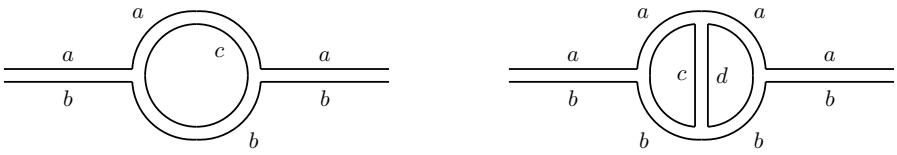

(a) The vertices bring a factor $(g/\sqrt{N})^2$ while the loop over the index c yields a factor N. The overall order of this diagram is $\mathcal{O}(g^2)$.

(b) The vertices bring a factor $(g/\sqrt{N})^4$ while the loops over the indices c, d yield a factor N^2. The overall order of this diagram is $\mathcal{O}(g^4)$.

Figure 1.5: One-loop and two-loop irreducible diagram contributions to the matrix model two-point function with equal input/output indices. We see that by dividing the loops, we can build diagrams with arbitrarily large order in g but at leading order in N. This is how the matrix model remains strongly coupled in the large-N limit.

AdS is topologically a cylinder whose boundary, while spatially infinitely far away, is causally connected with any inertial observer inside the spacetime — signals travelling at lightspeed can reach the boundary in finite time. This therefore means that we must set meaningful boundary conditions on fields living inside AdS. Through the GKPW formula, we see that these boundary conditions translate into sources for each operator in the CFT. This is illustrated in Fig. 1.6. The GKPW formula (1.11) is most useful in its saddle-point approximation. We have seen that the weakly coupled limit of the gravitational description corresponds to the large-N limit of the gauge description. Hence, on the CFT, the interesting saddle point is the large-N saddle-point of the path integral — which at large 't Hooft coupling remains a strongly coupled theory. On the gravitational side in the weak coupling limit, we are interested in a bulk configuration of fields which solves the Einstein field equations with boundary conditions set by the sources $h_i(x)$. The variation of this gravitational action w.r.t. the boundary values of the bulk fields will then yield the expectation values and various n-point correlators of the CFT in the large-N limit. In this limit, we have seen before that diagrams can get suppressed such that only a subset (which can be infinite in the strongly coupled case) survives. This will mean that only the contribution of operators whose diagrams survive at leading order will be accounted for and thus included in the gravitational bulk description.

Importantly, the GKPW formula makes no reference to its string theoretic top-down origin. This invites us to generalize it to a larger class of strongly coupled CFTs and simply engineer 'bottom-up' models where we only consider a minimal set of fields which are generally chosen by symmetries and phenomenological considerations and which we expect to be dominant in the large-N limit. This is fully in the spirit of CMT as we introduced in the first few pages of this introduction. It is this perspective we take when attempting to model non-quasiparticle physics in a quantum critical regime such as that of strange metals. One can study the strong coupling physics of scalar,

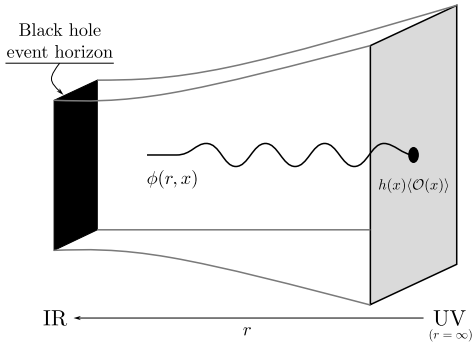

Figure 1.6: Schematic description of the AdS/CFT correspondence. We represent an asymptotically hyperbolic spacetime with a black hole event horizon in the interior in anticipation of finite temperature holography and with a bulk scalar field ϕ whose value at the conformal boundary $\phi(r=\infty,x)=h(x)$ sources a scalar operator $\langle\mathcal{O}\rangle$.

fermionic, vector operators in such theories by simply looking at semi-classical scalar, fermionic and vector fields in AdS. Throughout the various chapters of this thesis, we will be making use of this bottom-up approach in order to distil some knowledge about the low energy sector of strongly coupled CFTs.

Pushing the generalization further, one can deform any of these CFTs by a relevant operator which translates into a deformation of the AdS spacetime due to some matter/energy content. Remarkably when doing so, one finds that such solutions often stay within the weak gravity regime where the geometry from the boundary to the interior can be interpreted as an RG flow to a new (but still strongly coupled) infrared (IR) fixed point that can be computationally controlled. The *working hypothesis* of this thesis is that the new IR of these deformed holographic theories is sufficiently universal such that the theory can be used as an effective field theory for real-world systems with similar low energy physics. By this we mean that we assume that the RG flow in real, experimentally observed materials, starting at some microscopic ultraviolet (UV) fixed point set by the material itself, ends at some unknown strongly coupled IR fixed point characterized by some critical exponents (thermodynamical and dynamical). We then attempt to find another flow from a different, controlled, theoretical holographic UV fixed point which ends at a strongly coupled IR fixed point with the same exponents and low energy properties. By RG universality of critical phenomena, it is reasonable to conclude that those IR fixed points are the *same* low energy effective theories and thus the two separate flows belong to the same universality class. If so, we can use the theoretical model to explain experimental observations. This is illustrated in Fig. 1.7 where we draw a canonical example of universality — the Ising universality class describing very different models such as spins or gas molecules on a lattice — as well as the projected analogy for the strange metals.

1.3 Common holographic systems

In the previous sections, we have introduced the GKPW formula which relates operators of a CFT with fields in a gravitational dual, and we have motivated what type

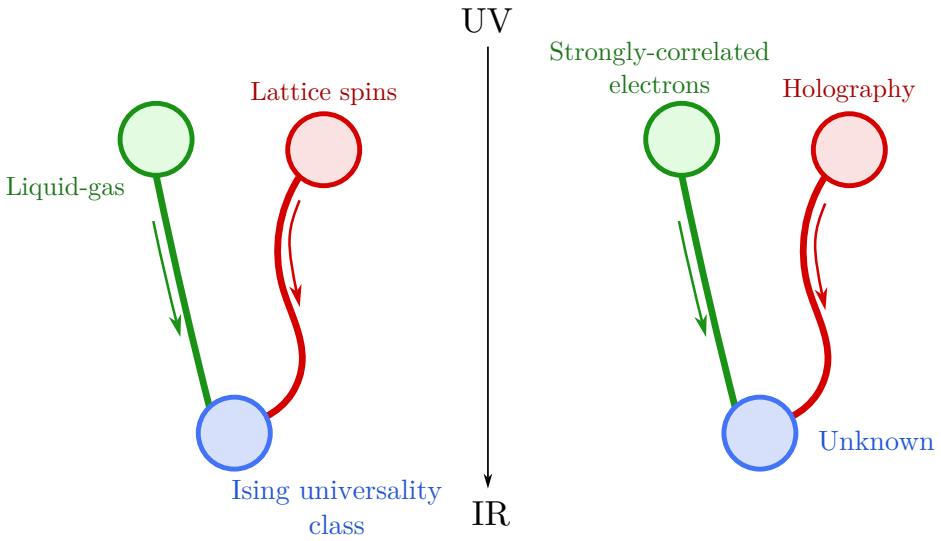

Figure 1.7: Left: Ising universality class describing the ferromagnet-paramagnet as well as the liquid-gas transitions. Right: Projected RG flow from the lattice UV fixed point describing the high-energy physics of strange metals (*e.g.*, cuprates) to some unknown IR theory. A holographic theory in the same universality class would flow to the same IR.

of CFTs should be studied with holography: CFTs deformed by a relevant operator that flow to a new yet still computationally accessible RG fixed point. We are now interested in detailing some common elements of bottom-up holographic models — these form a 'dictionary' of the duality (an excerpt of this dictionary can be found in Table 1.1).

The simplest AdS gravitational action one can write is the Einstein-Hilbert action with a negative cosmological constant Λ

$$S_{\text{EH}} = \frac{1}{2\kappa^2}\int \mathrm{d}^{d+2}x\sqrt{-g}\left[R - 2\Lambda\right] , \quad \Lambda = -\frac{d(d+1)}{2L^2} , \tag{1.12}$$

where we have made explicit the relation between the cosmological constant and the AdS curvature scale L.[7] The equations of motion for this action are solved by the AdS spacetime given by the metric[8]

$$\mathrm{d}s^2 = g_{\mu\nu}\mathrm{d}x^\mu \mathrm{d}x^\nu = \frac{L^2}{z^2}\left(\mathrm{d}z^2 - \mathrm{d}t^2 + \mathrm{d}x_i \mathrm{d}x^i\right) , \tag{1.13}$$

[7] In general, we rescale Λ to set $L = 1$.

[8] The Poincaré patch described by this solution does not cover the full AdS spacetime. It is however very convenient to describe QFTs in infinite volume since its conformal boundary is $\mathbb{R}^{1,d}$. We will make extensive use of this patch throughout the various chapters of this thesis

Boundary QFT	Bulk semi-classical gravity
Global symmetry	Local symmetry
Scalar operator $\mathcal{O}$	Bulk scalar field ϕ
Conformal dimension Δ of $\mathcal{O}$	Mass of the field ϕ
Source h of $\mathcal{O}$	Value of the leading branch $\phi_-(z=0)$
Expectation value $\langle\mathcal{O}\rangle$	Value of sub-leading branch $\phi_+(z=0)$
Correlator $\langle\mathcal{O}\mathcal{O}\rangle(\omega,k)$	Ratio $\frac{\delta\phi_+(z=0)}{\delta\phi_-(z=0)}$ for a linearized perturbation $\delta\phi e^{-i\omega t+ikx}$
CFT vacuum state	AdS solution
Thermal state	Black hole solution
Finite density state	Charged solution with gauge field A_t
Temperature	Hawking temperature
Entropy	Bekenstein-Hawking entropy
Chemical potential	Boundary value of A_t
Charge density	Boundary radial derivative of A_t
Free energy	On-shell regularized Euclidean action

Table 1.1: Excerpt of the holographic 'dictionary' prescriptions for bottom-up models.

where $z = 1/r$ is the radial coordinate and the conformal boundary (also named the UV boundary) is located at $z = 0$. The local isometry group of this spacetime is $SO(d+1,2)$, the conformal group in $d+1$ dimensions, which means that perturbations around this background will need to transform under representations of this group. Moreover, the AdS representations smoothly connect to conformal representations as one approaches the conformal boundary. Therefore, the CFT correlation functions we can compute out of this solution using the GKPW formula (1.11) transform covariantly under conformal symmetries and the state on the CFT-side of the duality will be the vacuum of a CFT_{d+1}.

Let us give an explicit example how to compute such GKPW correlation functions using a simple massive scalar field as a pedagogical model. In this example, we will only focus on the dynamics of the scalar field and ignore the metric, but everything we will show here is generally valid for all bulk fields, including the metric itself. The action on our bulk AdS_{d+2} is

$$S_{\text{scalar}} = -\int_M \mathrm{d}^{d+2}x\sqrt{-g}\left[\frac{1}{2}(\nabla\phi)^2 + \frac{m^2}{2}\phi^2\right] . \tag{1.14}$$

As we previously mentioned, we are interested in saddle-points of this action which can be found by varying the action w.r.t. ϕ

$$\delta S_{\text{scalar}} = \int_M \mathrm{d}^{d+2}x\sqrt{-g}\delta\phi\left(\nabla^2 - m^2\right)\phi - \oint_{\partial M}\mathrm{d}^{d+1}x\sqrt{-\gamma}\delta\phi N^z\partial_z\phi . \tag{1.15}$$

In this computation, we have integrated by parts the bulk integral yielding the first term, proportional to the equation of motion. A saddle-point solution will therefore solve the Klein-Gordon equation of motion *i.e.*, $\left(\nabla^2 - m^2\right)\phi(z) = 0$ (from here on, we assume that the scalar field only depends on the radial coordinate, which in pure AdS is sufficient due to separation of variables). The second term is a remaining boundary integral after integrating by parts. In this boundary term, γ is the induced metric on the boundary and N^μ is an outward-pointing unit vector defining the boundary hypersurface[9]. Near the UV boundary, the Laplacian operator in the radial direction takes the form $\nabla^2\phi \sim z^2\partial_z^2\phi - d\, z\partial_z\phi$ such that the scalar field admits the follow expansion

$$\phi(z) \sim \phi_-(z) z^{d+1-\Delta} + \phi_+(z) z^\Delta + \dots \,, \tag{1.16}$$

where Δ is the larger solution of $\Delta(\Delta - d - 1) = m^2$ *i.e.*,

$$\Delta = \frac{d+1}{2} + \frac{1}{2}\sqrt{(d+1)^2 + m^2} > \frac{d+1}{2} \,. \tag{1.17}$$

The two independent branches $\phi_\pm$ then yield two degrees of freedom $\phi_\pm^{(0)} = \phi_\pm(z=0)$ whereas the higher order terms in their expansions are constrained by the equations of motion. Near the boundary, we will also be using that $N^z \sim -\sqrt{g^{zz}} \sim -z$ such that we can then compute the on-shell variation of the action (1.15)

$$\begin{aligned} \delta S_{\text{scalar}} &= \oint_{\partial M} \mathrm{d}^{d+1}x z^{-d} \left(\delta\phi_-^{(0)} z^{d_\Delta} + \delta\phi_+^{(0)} z^\Delta\right)\left[d_\Delta \phi_-^{(0)} z^{d_\Delta - 1} + \Delta\phi_+^{(0)} z^{\Delta-1}\right] \\ &= \oint_{\partial M} \mathrm{d}^{d+1}x \left[d_\Delta \phi_-^{(0)}\delta\phi_-^{(0)} z^{d_\Delta - \Delta} + \left(\Delta\phi_+^{(0)}\delta\phi_-^{(0)} + d_\Delta\phi_-^{(0)}\delta\phi_+^{(0)}\right) + \dots\right] \,. \end{aligned} \tag{1.18}$$

Here we defined $d_\Delta = d + 1 - \Delta$. Since $\Delta > \frac{d+1}{2}$, then $d_\Delta - \Delta < 0$ and the first term diverges as $z \to 0$. To quell this divergence, we can add an extra boundary term to (1.14) which will not change the equations of motion and will only regularize the action in the boundary — we will discuss this topic in further generality in chapter 4. The extra boundary term[10] we consider is then

$$S_{\text{bdy,scalar}} = \oint \mathrm{d}^{d+1}x\sqrt{-\gamma}\frac{m_0^2}{2}\phi^2 \,, \tag{1.19}$$

whose variation leads to an extra contribution

$$\delta S_{\text{bdy,scalar}} = m_0^2 \oint_{\partial M} \phi_-^{(0)}\delta\phi_-^{(0)} z^{d_\Delta - \Delta} + \phi_+^{(0)}\delta\phi_-^{(0)} + \phi_-^{(0)}\delta\phi_+^{(0)} + \dots \tag{1.20}$$

[9] In the coordinate system (1.13), the normal vector to the boundary hypersurface N^μ can be chosen such that only the component N^z is non-zero.

[10] A priori we could consider other boundary terms which might simply not contribute at leading order *i.e.*, irrelevant deformations or, depending on the value of the mass m^2, we can use a boundary term which would reverse the roles of $\phi_-^{(0)}$ and $\phi_+^{(0)}$ *i.e.*, a Legendre transformation. Chapter 4 has an in-depth discussion of this point.

By choosing $m_0^2 = -d_\Delta$, the leading divergent term vanishes and we are left with a finite contribution proportional to $\phi_+^{(0)}\delta\phi_-^{(0)}$ plus terms that vanish as $z \to 0$. The total finite variation becomes

$$\delta S_{\text{scalar}} = \left(2\Delta - d - 1\right) \oint_{\partial M} \mathrm{d}^{d+1}x\, \phi_+^{(0)}\delta\phi_-^{(0)} \,. \tag{1.21}$$

This term can be written as $\delta S = \oint \langle \mathcal{O} \rangle \delta h$ where we identify $\delta h = \delta\phi_-^{(0)}$ as the source of the bulk scalar field following the GKPW description.[11] Through the GKPW formula (1.11) and in the saddle-point approximation, computing the variation of the action S_{scalar} is the same as computing the expectation value of the associated QFT operator

$$\frac{\delta S_{\text{scalar}}}{\delta h} = -i\frac{\delta}{\delta h}\log Z_{\text{QFT}} = \langle \mathcal{O} \rangle \,. \tag{1.22}$$

So we deduce here that the expectation value of the QFT scalar operator associated with the bulk field ϕ is $\langle \mathcal{O} \rangle = \left(2\Delta - d - 1\right)\phi_+^{(0)}$. This relation between the falloffs of the bulk field and the boundary source and expectation value of the associated operator is at the core of the AdS/CFT duality. Pushing this reasoning further, we can similarly compute the n-point correlation functions of the QFT operator $\mathcal{O}$. Taking the two-point correlator as an example, we use that within linear response theory and in Fourier space, $\langle \mathcal{O}(\omega,k) \rangle = G_{\mathcal{O}\mathcal{O}}(\omega,k)\delta h(\omega,k)$. So to obtain the two-point function, one must simply add to the saddle-point solution ϕ a plane wave perturbation $\delta\phi(z)e^{-i\omega t + ikx}$, solve the linearized equations of motion for this model with Dirichlet boundary conditions and finally read off the Green's function through the ratio

$$G_{\mathcal{O}\mathcal{O}}(\omega,k) = \left(2\Delta - d - 1\right)\frac{\delta\phi_+^{(0)}}{\delta\phi_-^{(0)}} \,. \tag{1.23}$$

We can now build on the knowledge of how to compute correlation functions in the conformal vacuum to deduce how to generalize this computation to other states. As we have just seen, the choice of sources of operators on the QFT fixes the boundary conditions on the bulk fields in the UV region. The boundary conditions deep in the interior can still be chosen freely. This allows for multiple solutions which we will consider as different states of the theory. An intuitive way to see this is to remember that the radial coordinate encodes for the RG flow such that the IR of the theory corresponds to the low energy sector of the dual QFT where state specific aspects become important. For instance, the Anti-de Sitter-Schwarzschild (AdS-Schw) black hole solution can be obtained by allowing for a more general metric ansatz and requiring that g_{tt} vanishes for some value $z = z_h$, which defines the black hole event horizon.

[11] In the initial section of this chapter, we have mentioned that the correspondence maps the source to the boundary value of the bulk field, whereas we now show that it is actually given by the coefficient of the term scaling as $z^{d+1-\Delta}$. In practice, one often works with rescaled fields $\varphi = z^{\Delta-d-1}\phi$ such that the sourcing is done by imposing Dirichlet boundary conditions on φ.

This solution takes the following form

$$\mathrm{d}s^2 = \frac{L^2}{z^2}\left(\frac{\mathrm{d}z^2}{f(z)} - f(z)\mathrm{d}t^2 + \mathrm{d}x_i\mathrm{d}x^i\right), \quad f(z) = 1 - \left(\frac{z}{z_h}\right)^{d+1}. \tag{1.24}$$

What states could this encode in the QFT? Black holes naturally introduce a notion of thermodynamics in the system with their Hawking temperature T [28] and Bekenstein-Hawking entropy S [29], and it is thus reasonable to conclude that the dual state to this AdS-Schw solution is a CFT thermal state. The thermodynamic quantities can be read off from the geometry near the horizon; the temperature is given by the slope of the emblackening factor f at the horizon $T = \frac{-f'(z_h)}{4\pi}$ while the entropy density is given by the area density of the event horizon $s = 4\pi\sqrt{\prod_i g_{ii}(z_h)}$ (where the product is defined on the d spatial coordinates). Many subsequent tests have verified that this identification is correct [30].

Two different solutions to the same equations of motion will yield two different holographic states, yet in general we are interested in the thermodynamically preferred state of a system. In this case, we select the solution which minimizes the free energy of the system. By definition, the free energy is related to the Euclidean partition function through $F = -T\log Z^E_{\mathrm{QFT}}$ which, when using the GKPW formula (1.11) and when the collective bulk fields ϕ are taken on a saddle-point ϕ_0, can be related to the Euclidean on-shell gravitational action

$$F = TS^{E,\mathrm{reg.}}_{\mathrm{grav.}}[\phi = \phi_0]\,. \tag{1.25}$$

This notion of thermodynamics is fully compatible with the black hole thermodynamics of the AdS-Schw solution such that the integrated first law of thermodynamics is obeyed $F = E - TS$ (where E is the internal energy of the solution obtained by reading the expectation value of the boundary quantity dual to the bulk metric field).[12]

To construct another state which we will use heavily, we need to introduce the electromagnetic charge. These are associated with a local $U(1)$ symmetry (this is notably the case for the ordinary electric charge). In condensed matter applications however, one can usually ignore the dynamics of the electromagnetic field and only think of the symmetry as a global $U(1)$ describing conserved particle flows. An important feature of holography is that it maps global symmetries to local symmetries. The argument behind this statement can be readily understood by considering some local gauge symmetry in the bulk — the diffeomorphism invariance of general relativity

[12] In the expression (1.25), an extra regularization constraint was imposed on the Euclidean gravitational action. The reason behind this is that bulk actions in holography are usually supplemented with two kinds of boundary integrals — the first kind, which we previously discussed, is required to make the variational problem on the boundary well-defined while the second kind consists of counterterms to regularize UV divergences. These additions only have support on the boundary, and therefore they do not affect the bulk equation of motions and their solutions. However, they play a vital role when varying the action around a saddle-point as we will see shortly. These two types of contributions will be thoroughly reviewed for a specific holographic model in chapter 4.

for instance. Variations of the total action — meaning (1.12) and additional boundary terms — can formally be written as[13]

$$\delta S = \int \mathrm{d}^{d+2}x\sqrt{-g}\Big(R_{\mu\nu} - \frac{2\Lambda}{d}g_{\mu\nu}\Big)\delta g^{\mu\nu} + \oint \mathrm{d}^{d+1}x\sqrt{-\gamma}T^{\mu\nu}\delta g_{\mu\nu}\ , \tag{1.26}$$

where the bulk term is proportional to the equations of motion which vanishes on-shell and γ is once again the induced metric determinant on the boundary. Applying the same logic we previously used for the scalar field action, we can conclude that $T_{\mu\nu}$ is the boundary expectation value associated with the QFT source $\delta g^{\mu\nu}$. Let us now consider a diffeomorphism transformation on the metric variation $\delta g_{\mu\nu} \to \delta g_{\mu\nu} + \nabla_\mu \xi_\nu + \nabla_\nu \xi_\mu$ for some vector ξ. Requiring that δS is invariant under such gauge transformation is equivalent to the condition

$$\oint \mathrm{d}^{d+1}x\sqrt{-\gamma}T^{\mu\nu}\nabla_\mu\xi_\nu = -\oint \sqrt{-\gamma}\xi_\nu\nabla_\mu T^{\mu\nu} = 0\ . \tag{1.27}$$

To obtain this equality, we used that $\sqrt{-g}\nabla_\mu X_\nu = \partial_\mu\left(\sqrt{-g}X_\nu\right)$, and we integrated by parts. The condition (1.27) must be valid for every vector ξ and thus is equivalent to the conservation equation $\nabla_\mu T^{\mu\nu} = 0$. A more detailed argument shows that $T^{z\mu}$ can also be set to zero and, noting that the AdS metric is flat at the conformal boundary, we therefore have on the boundary theory $\partial_i T^{ij} = 0$ — thus indicating that T_{ij} is the boundary stress-tensor.[14]

This feature tells us that in order to introduce a conserved $U(1)$ current in the boundary, we must add a local $U(1)$ gauge field A_μ in the bulk. The minimal extension to the Einstein-Hilbert action with such a gauge field is the Einstein-Maxwell action

$$S_{\mathrm{EM}} = S_{\mathrm{EH}} - \frac{1}{4e^2}\int \mathrm{d}^{d+2}x\sqrt{-g}F_{\mu\nu}F^{\mu\nu}\ , \quad F_{\mu\nu} \equiv \partial_\mu A_\nu - \partial_\nu A_\mu\ . \tag{1.28}$$

The canonical black hole saddle-point for this action is the Reissner-Nordström (RN) charged black hole solution which uses the same metric ansatz as (1.24) but with a different emblackening factor as well as a non-trivial gauge field

$$f(z) = \left(1 - \frac{z}{z_h}\right)\left(1 + \frac{z}{z_h} + \frac{z^2}{z_h^2} - \frac{\mu^2 z^3}{4z_h}\right)\ , \quad A = \mu\left(1 - \frac{z}{z_h}\right)\mathrm{d}t \quad (\text{in } d = 2). \tag{1.29}$$

This family of solutions is parametrized by (μ, z_h) where now μ is the boundary value of A_t and therefore the source of the charge density operator $J^t = n$ on the boundary

[13] Here we see immediately why boundary terms must be supplemented to (1.12). In this specific example, we consider Dirichlet boundary conditions on the metric, and therefore we must eliminate any leftover variations proportional to $\partial_z \delta g_{\mu\nu}$ which naturally arise when varying the Ricci scalar. This can be done using the Gibbons-Hawking-York term [31]. Counterterms are also needed to tame the divergences in the volume element $\sqrt{-g} \sim z^{-(d+2)}$ near the boundary.

[14] An important consequence of this statement is that the bulk stress-energy tensor in the gravitational system, defined as the r.h.s. of the Einstein equations $R_{\mu\nu} - \frac{1}{2}(R - 2\Lambda)g_{\mu\nu} = \kappa^2 \hat{T}_{\mu\nu}$, is fundamentally different from the boundary stress-energy tensor.

theory — μ can thus be identified as the chemical potential of the boundary theory. This allows us to deduce that this solution encodes for a thermal finite density QFT whose thermodynamics will now obey the first law of thermodynamics $F = E - TS - \mu N$, where the free energy F can once again be obtained by the Euclidean on-shell regularized gravitational action.

Such a solution, parametrized only by a temperature and a finite density, has garnered a lot of interest over the years for condensed matter applications, as its near-horizon geometry encoding for low energy physics shows a novel heretofore unknown IR anchored on an emergent $\mathrm{AdS}_2 \times \mathbb{R}^2$ geometry [32, 33]. This was immediately recognized as the dual of a quantum critical sector in the spectrum of the theory, with curiously an infinite dynamical critical exponent $\mathbf{z} = \infty$.[15]

More generalized types of scaling can be found from the infrared geometry of more complicated black hole solutions [32, 34, 35, 36]. The most general family of such solutions are saddle-points of the Einstein-Maxwell-Dilaton (EMD) action

$$S_{\mathrm{EMD}} = \int \mathrm{d}^{d+2}x\sqrt{-g}\left[\frac{1}{2\kappa^2}(R-2\Lambda) - \frac{Z(\phi)}{4e^2}F_{\mu\nu}F^{\mu\nu} - \frac{1}{2}(\partial\phi)^2 - V(\phi)\right], \tag{1.30}$$

where V and Z are arbitrary functions of ϕ. These solutions will yield a near-horizon geometry of the form

$$\mathrm{d}s^2 = r^{2\theta/d}\left[-\frac{\mathrm{d}t^2}{r^{2\mathbf{z}}} + \frac{\mathrm{d}r^2 + \mathrm{d}x_i\mathrm{d}x^i}{r^2}\right] \tag{1.31}$$

where we have set $L = 1$ and the horizon is now located at $r \to 0$. The exact choice of scalar potentials V, Z will determine the value of the exponents $\theta, \mathbf{z}$. We have already encountered $\mathbf{z}$, identified as the dynamical critical exponent of a quantum critical theory, and θ can be identified as the hyperscaling violation exponent.[16] Since the scalings control the IR geometry of the theory where the event horizon lies, they will directly affect the low temperature thermodynamic scalings, with in particular the entropy density obeying a scaling form $s \sim T^{\frac{d-\theta}{\mathbf{z}}}$.

As we mentioned previously, the near-horizon geometry of the RN solution is $\mathrm{AdS}_2 \times \mathbb{R}^2$. We can deduce from Eq. (1.31) that for the RN black hole, the two exponents take the values $(\theta, \mathbf{z}) = (d, \infty)$. An immediate consequence of this scaling is that for the RN solution, $S(T \to 0) = S_0 > 0$. This finite ground state entropy signals that the RN solution is a fine-tuned point in the large-N limit and will carry artifacts of such limit. By the usual arguments, it should be unstable. Let us set aside that matter for a second and focus on the intriguing property of an infinite dynamical critical

[15] The existence of such a state has later been verified for SYK-type models, confirming that this feature is not a holographic artifact.

[16] While the dynamical critical exponent relates scaling properties of space and time, the hyperscaling violation exponent sets an effective dimensionality $d_{\mathrm{eff.}} = d - \theta$ for the system at low energies. A typical example of such property can be found in theories with a Fermi surface which are effectively one-dimensional and whose physics is set by a non-decoupling dimensionful energy scale: the Fermi energy.

exponent $\mathbf{z} = \infty$. Remembering the physics of QCPs of the previous section, an infinite dynamical critical exponent means that the system remains in the quantum critical regime throughout a large portion of parameter space (this is akin to having a flat cone for the quantum critical regime). This suggests that the RN solution is closer to describing a quantum critical phase rather than a quantum critical point. Moreover, in that limit, lengths and spatial momenta do not scale away at low energies and thus any momentum can contribute to low energy fluctuations. This seems to hint that, in spite of its fine-tuning, the RN solution demonstrates relevant physics to that of strange metals. Other solutions were later found which also displayed an infinite critical dynamical exponent $\mathbf{z} = \infty$ while preserving the third law of thermodynamics. This is made possible when the hyperscaling violation exponent also diverges while keeping the ratio $-\frac{\theta}{\mathbf{z}} \equiv \eta$ fixed. The near-horizon geometry is then *conformal-to-AdS*$_2$ *i.e.*, it is related to the near-horizon RN geometry by a conformal factor as [37]

$$\mathrm{d}s^2 = y^{-\frac{2\eta}{\eta+d}} \left[a^2 \frac{-\mathrm{d}\tilde{t}^2 + \mathrm{d}y^2}{y^2} + \mathrm{d}x_i \mathrm{d}x^i \right] , \quad a = \frac{d}{\eta + d} \mathbf{z}^{-1} , \tag{1.32}$$

where we used the coordinate transformation $r \to y^a$ and $t \to a\tilde{t}$ on (1.31) and used that $a - 1 \sim -1$ as $\mathbf{z} \to \infty$. Such near-horizon geometries will then lead to entropy scalings $S \sim T^\eta$ which will vanish at low temperatures for $\eta > 0$. Among this family of solutions, we will be interested in this thesis in the Gubser-Rocha (GR) model [38] which has $\eta = 1$ and therefore an entropy $S \sim T$, the same scaling behavior observed in a Fermi liquid (which has $(\mathbf{z}, \theta) = (1, d-1)$). Note that in practice, while these more refined solutions provide a less artificial starting point to study $\mathbf{z} \to \infty$ physics than the RN solution, they are also generally more complicated. For that reason, it is still common to study the RN solution as a simpler toy model and eventually consider a conformal-to-AdS$_2$ model as a refinement — which is what we will do in chapter 2.

1.4 This thesis

In this introduction, we have presented a pedagogical review of the tools and ideas behind the AdS/CFT correspondence with a strong emphasis on its application to study strongly correlated quantum matter at novel QCPs and QCPh's. In the following chapters of this thesis, we will apply these methods to various holographic models built in order to produce varied physics, showcasing the universal power of our holographic methods for such cases, either in the direction of experimental strange metals or to address more fundamental theoretical puzzles. These applications can be grouped in three parts.

1.4.1 Chapters 2, 3, 4 — Metallic transport in an ionic lattice

We will follow this introduction with chapter 2 in which we will numerically construct black hole solutions with modulated boundary charge densities in order to simulate the effect of a lattice made of background ions on the holographic QCPh of

the RN and GR models. Chapter 2 will further feature a detailed introduction of the wider condensed matter context and will situate our findings within that context. Our numerical data will allow us to measure electrical and thermal conductivities, thus probing flows of charge and thermal carriers in such a modulated potential, both at small *i.e.*, perturbative, and at large lattice potential strength. These observables can be directly compared with laboratory experiments and are thus of great interest.

The holographic data in the perturbative regime at small wavelength and frequencies will then be thoroughly compared with the theoretical predictions of a purely hydrodynamic flow of electric charges with perturbatively small spatial modulation of their chemical potential. The general framework of the underlying hydrodynamic theory will be developed in chapter 3 where we present a novel, standalone hydrodynamic calculation. The benefit of such theories comes from the wide range of systems they can describe. However, as effective theories, they lack predictive power without microscopic model-specific input. We will thus further see in chapter 3 that holography doubles as a great set of microscopic models to probe interesting hydrodynamic behavior. Why hydrodynamics gives additional theoretical leverage to describe QCPh's will be explained.

The question of the quantization procedure on the QFT side of the duality for the GR solution (with or without a lattice modulation) is a subtle but important detail of the GKPW formula that we have so far not addressed and can often be ignored. However, for the GR model which we considered for experimental reasons, one cannot ignore this subtlety. In particular, one must carefully understand the role of the scalar field in the action (1.30) under the flow of the Renormalization Group in order to interpret the boundary theory, as well as to understand its influence on the choice of sources imposed as boundary conditions when computing correlation functions. In chapter 4, we will derive the various interpretations of the boundary theory and a posteriori justify the choices of boundary conditions made in chapter 2.

1.4.2 Chapter 5 — Regulated Quantum Electron Star

An interesting feature of black holes in AdS is that they can be 'hairy' *i.e.*, they can be labelled by more than just their mass, charge and angular momentum. This was rather unexpected and counter to much of the conventional flat space gravitational wisdom at the time but proved to be an essential feature of the AdS/CFT correspondence. It was shown that scalars readily condensate around a black hole. This is the dual to some scalar order parameter condensating in the boundary QFT and indicating a phase transition to some broken symmetry phase. When the scalar is charged under the $U(1)$ local gauge symmetry, the condensed state is similar to a superconducting state[17] around a quantum critical metal; in other words, the holographic superconductor [39, 40, 41].

[17] Formally it is only a superfluid as the broken $U(1)$ symmetry is a global symmetry of the boundary.

Fermions proved more difficult. Due to the Pauli principle, they do not condensate and thus initially, all that was observed was an instability of the black hole solution under light fermionic perturbations. By considering the density of fermions to be high enough, it was possible to treat them as an effective charged fluid — similar to a neutron star but with charge — leading to an AdS electron star solution [42]. While it was hoped that this solution would shed some light on the physics of strongly interacting fermionic systems, it also displayed some artifacts of the holographic origin of this theory, therefore failing the hypothesis of universal emergent low energy features. In more detail, the electron star showed an infinite amount of Fermi surfaces in its spectrum, a remnant of the large-N limit saddle-point approximation. Further attempts were then made to study this question in more sophisticated ways in order to shield the IR from purely holographic effects [43, 44, 45, 46] until eventually the assumption of large density was found to be the cause of these spurious Fermi surfaces. New attempts were made [47, 48, 49, 50] at reaching the other end of the spectrum, characterized by a small density of fermions where quantum corrections might be required. These new models were free of the holographic effects but lost the semiclassical gravitational stability of the electron star. In chapter 5 of this thesis, we will provide a new model attempting to bridge these two concepts — a model of a quantum electron star which is both gravitationally and thermodynamically stable while only displaying a single Fermi surface — at the price of introducing some external regulator in the form of a non-dynamical scalar field.

1.4.3 Chapter 6 — Nielsen complexity of conformal field theories

The last chapter of this thesis will look at strongly coupled systems from a different point of view. A crucial observation is that there seems to be a deep connection between the notions of strong coupling in QFTs and long-range entanglement, see *e.g.*, [51]. The main idea behind this statement is that when interactions are weak, it is expected that each part of the system only overlaps with its neighbors and the resulting entanglement pattern should be short-range. However, with strong interactions, a small part of the system can reach further away from its local support which leads to long-range densely entangled states. The QCPs we have been discussing are themselves examples of such states; since they are described by CFTs, the entanglement structure of a given subregion will diverge logarithmically in the length of the subregion [52]. This observation was the impetus behind the search for a holographic quantity encoding this property of strongly interacting systems. The first result of this kind was the discovery by Ryu and Takayanagi of a geometric quantity matching the entanglement entropy of a CFT subregion [53]. This result was inspired by the Bekenstein-Hawking entropy formula, yet instead of equating the entanglement entropy to the area of the event horizon of a black hole, it is given by the area of an extremal surface anchored at the UV boundary on the subregion.

However, the interior region of a black hole is never probed by such extremal surfaces and therefore a priori not accounted by this subsystem entanglement entropy.

It was then an affirmation that entanglement entropy (and the various analogous proposals for mixed states of bipartite systems) is not enough to account for the entire entanglement structure of a system [54, 55].

Recent efforts have been made to bridge that gap from the boundary side by finding another quantity which would probe deeper into the entanglement pattern of QFTs. One such attempt is called 'Nielsen complexity' [56, 57, 58]. This was inspired by the field of quantum computing wherein the complexity of a given unitary operation is measured by the minimal number of elementary operations required to build it. In quantum systems and more generally QFTs, Nielsen proposed that this discrete measure should generalize to a distance in the space of unitaries. While there is no doubt that such a quantity can be a useful measure, many ambiguities in its definition remain (such as the choice of gate set and cost functions). In chapter 6, we study one such possible measure on CFTs in various dimensions, and, through the holographic duality, directly and unambiguously connect it to the dynamics of massive semiclassical particles in AdS.